

This is a repository copy of *Geometric morphometrics and finite elements analysis : Assessing the functional implications of differences in craniofacial form in the hominin fossil record*.

White Rose Research Online URL for this paper:

<https://eprints.whiterose.ac.uk/127295/>

Version: Accepted Version

Article:

O'Higgins, Paul orcid.org/0000-0002-9797-0809, Fitton, Laura C. orcid.org/0000-0003-4641-931X and Godinho, Ricardo Miguel (2017) Geometric morphometrics and finite elements analysis : Assessing the functional implications of differences in craniofacial form in the hominin fossil record. *Journal of archaeological science*. ISSN 0305-4403

<https://doi.org/10.1016/j.jas.2017.09.011>

Reuse

Items deposited in White Rose Research Online are protected by copyright, with all rights reserved unless indicated otherwise. They may be downloaded and/or printed for private study, or other acts as permitted by national copyright laws. The publisher or other rights holders may allow further reproduction and re-use of the full text version. This is indicated by the licence information on the White Rose Research Online record for the item.

Takedown

If you consider content in White Rose Research Online to be in breach of UK law, please notify us by emailing eprints@whiterose.ac.uk including the URL of the record and the reason for the withdrawal request.

Geometric morphometrics and Finite elements analysis: Assessing the functional implications of differences in craniofacial form in the hominin fossil record

Paul O'Higgins^a, Laura C Fitton^a and Ricardo Miguel Godinho^a

Paul O'Higgins (corresponding author)

a) Hull York Medical School and Department of Archaeology of the University of York

John Hughlings Jackson Building, University of York, Heslington, York YO10 5DD, UK

paul.ohiggins@hyms.ac.uk

Laura C. Fitton

Hull York Medical School and Department of Archaeology of the University of York

John Hughlings Jackson Building, University of York, Heslington, York YO10 5DD, UK

laura.fitton@hyms.ac.uk

Ricardo Miguel Godinho¹

a) Hull York Medical School and Department of Archaeology of the University of York

Academic address: John Hughlings Jackson Building, University of York, Heslington, York

YO10 5DD, UK

b) Interdisciplinary Center for Archaeology and Evolution of Human Behaviour (ICArHEB)

Faculdade das Ciências Humanas e Sociais, Universidade do Algarve, Campus Gambelas,

8005-139, Faro, Portugal

¹ Permanent address: R. Dr. Joaquim Fiadeiro, nº86, Urbanização Tapada do Carapetal, 7200-480 Reguengos de Monsaraz, Portugal

23 ricardomiguelgodinho@gmail.com

24

25

26 **Abstract:**

27 The study of morphological variation in the hominin fossil record has been transformed in
28 recent years by the advent of high resolution 3D imaging combined with improved geometric
29 morphometric (GM) toolkits. In parallel, increasing numbers of studies have applied finite
30 elements analysis (FEA) to the study of skeletal mechanics in fossil and extant hominoid
31 material. While FEA studies of fossils are becoming ever more popular they are constrained
32 by the difficulties of reconstruction and by the uncertainty that inevitably attaches to the
33 estimation of forces and material properties. Adding to these modelling difficulties it is still
34 unclear how FEA analyses should best deal with species variation.

35 Comparative studies of skeletal form and function can be further advanced by applying tools
36 from the GM toolkit to the inputs and outputs of FEA studies. First they facilitate virtual
37 reconstruction of damaged material and can be used to rapidly create 3D models of skeletal
38 structures. Second, GM methods allow variation to be accounted for in FEA by warping
39 models to represent mean and extreme forms of interest. Third, GM methods can be applied
40 to compare FEA outputs – the ways in which skeletal elements deform when loaded. Model
41 comparisons are hampered by differences in material properties, forces and size among
42 models but how deformations from FEA are impacted by these parameters is increasingly
43 well understood, allowing them to be taken into account in comparing FEA outputs.

44 In this paper we review recent advances in the application of GM in relation to FEA studies
45 of craniofacial form in hominins, providing examples from our recent work and a critical
46 appraisal of the state of the art.

47

48 **Keywords:** Form-function; Geometric Morphometrics; Finite Element Analysis; Craniofacial
49 form; Functional performance.

50

1. Introduction

In this paper we consider how the mechanical performance of crania in biting can be estimated and compared among fossils, paying particular attention to how the methods of geometric morphometrics (GM) can facilitate such analyses in combination with biomechanical modelling using finite elements analysis (FEA).

As with other skeletal elements, crania fulfil mechanical functions, such as housing and protection of organs and provision of a rigid framework for food acquisition and intra-oral processing by the masticatory apparatus (Lieberman, 2011), which comprises jaws, teeth and soft tissues. Thus, much research has focused on the association between cranial form and masticatory function, with the aims of understanding how crania function and how their functional abilities (performances) differ among related species. These differences have underpinned investigations of how skeletal form, function, ecology and behaviour interrelate (Groning, et al., 2011b, Rayfield, 2005, Rayfield, 2007, Rayfield, et al., 2001, Strait, et al., 2010, Strait, et al., 2007, Strait, et al., 2009, Wroe, et al., 2010, Wroe, et al., 2007). In turn, knowledge of these interrelationships has been used to infer ecology and behaviour from skeletal remains of extinct taxa (Attard, et al., 2014, Cox, et al., 2015, Degrange, et al., 2010, Ledogar, et al., 2016, Oldfield, et al., 2012, Rayfield, 2005, Rayfield, et al., 2001, Smith, et al., 2015b, Strait, et al., 2010, Strait, et al., 2009, Wroe, 2008).

One aspect of performance, bite force, can be directly measured in extant species using force transducers. These have been widely used to measure bite forces in living humans (Braun, et al., 1995, Kikuchi, et al., 1997, Paphangkorakit and Osborn, 1997, Sinn, et al., 1996). In extinct material alternative approaches are required to estimate forces from skeletal evidence, using bony proxies to approximate lever arm lengths and maximum muscle forces based on the relationships between muscle area, intrinsic muscle fibre strength and force production (Gans and de Vree, 1987, Josephson, 1975, Weijs, 1980). Although this provides an estimate of the force produced by muscles it ignores pennation and depends on the validity of the estimates of muscle areas from bony proxies. Muscle force is converted into bite force through the masticatory lever arm system. By measuring in and out-levers of the masticatory system and computing their ratios, it is possible to estimate the mechanical efficiencies of each muscle and to estimate maximal bite forces (Antón, 1990, Demes and Creel, 1988, Eng,

et al., 2013, O'Connor, et al., 2005). However, this approach has limitations due to differences between the cross sectional areas estimated via bony proxies and actual physiological muscle cross sectional areas (Eng, et al., 2013, Toro-Ibacache, et al., 2015), and because the lever system of the jaws is often simplified to two dimensions to ease calculations. Bite force can also be predicted using FEA (Wroe, et al., 2010) and by multibody dynamic analysis (MDA) (Bates and Falkingham, 2012, Curtis, et al., 2008, Shi, et al., 2012). MDA can also be used to infer muscle activation patterns given a particular load. These approaches take full account of the three dimensional geometry of the masticatory lever system but retain dependence on the accuracy of input of variables, such as muscle forces, force vector directions and cranial geometry.

Bite forces are transmitted to items held between the teeth, and the teeth and cranium experience the bite reaction force. Thus, crania have to be adapted to withstand masticatory forces. In order to assess, explain and compare how the cranium resists occlusal forces, researchers have used several approaches. These include the analysis of simplified biomechanical models of craniofacial anatomy considered in terms of vertical and horizontal column-like structures that buttress the face and channel bite reaction forces (Görke, 1904; Richter, 1920; Endo, 1965; Endo, 1966) and models that consider crania as a cylinder that is twisted during biting (Greaves, 1985; Greaves and Mucci, 1997; Demes, 1987). These models and their underlying assumptions have been tested through the application of strain gauges to directly measure the surface strains experienced during biting (Hylander et al., 1991; Hylander et al., 1992; Ross and Hylander, 1996; Ravosa et al., 2000a; Ravosa et al., 2000b; Ross, 2001; Ross et al., 2011). FEA has also been applied to this task (Ledogar, et al., 2016, Smith, et al., 2015b, Strait, et al., 2010, Strait, et al., 2007, Strait, et al., 2009, Wroe, et al., 2010) but an important issue in such studies is validity of FEA results, do they match reality?

For this reason validation studies have been carried out to assess the accuracy of prediction of cranial and mandibular deformations, comparing measured with predicted strains (Bright and Groning, 2011, Groning, et al., 2009, Kupczik, et al., 2007, Ross, 2005, Toro-Ibacache, et al., 2016). In so doing, researchers can assess how various input parameters including skeletal geometry, material properties, constraints, applied forces etc. impact FE model results in order to create more realistic models (Ross, 2005, Strait, et al., 2005, Toro-Ibacache, et al., 2016). In general validation studies tell us that accurate strain prediction in any one specimen is difficult and requires careful adjustment of model parameters to achieve valid results.

The accuracy of predictions achieved by FEA is, however, entirely dependent on these input parameters, so, acknowledging modelling limitations, researchers have sought to understand the impact of variations and simplifications in FE modelling. This has led to sensitivity studies in which the impact on predicted deformations of varying specific parameters is assessed. Such parameters include the muscle force magnitudes, directions and activation patterns (Cox, et al., 2011, Fitton, et al., 2012, Groning, et al., 2012, Ross, 2005, Sellers and Crompton, 2004), variations in material properties (Cox, et al., 2011, Groning, et al., 2012, Kupczik, et al., 2007, Reed, et al., 2011, Strait, et al., 2005, Toro-Ibacache, et al., 2016), modelling cranial sutures (Kupczik, et al., 2007, Reed, et al., 2011, Wang, et al., 2010), simplifications in model geometry (Fitton, et al., 2015, Toro-Ibacache, et al., 2016), modelling the periodontal ligament (Groning, et al., 2012, Holland, 2013, McCormack, et al., 2014, Wood, et al., 2011), impact of variations in modelling of trabecular bone (Parr, et al., 2013) and model constraints (Cox, et al., 2011). Validation and sensitivity studies have shown that modelling variations that affect model stiffness (e.g. bone thicknesses, how cancellous bone is represented, material properties, etc.) or total applied force tend to lead to differences in magnitude rather than mode of deformation, while variations in relative muscle activations, muscle vectors and constraints tend to impact mode of deformation, how the cranium deforms (Fitton, et al., 2015, Godinho, et al., 2017, Parr, et al., 2012, Toro-Ibacache, et al., 2016).

Researchers have tried to predict how fossil hominin crania resist biting. Such analyses have until recently relied on geometrical simplifications of crania (Demes, 1987, Rak, 1983, Rak, 1986, Trinkaus, 1987). More recently, FEA has been used to more fully model fossil hominin masticatory biomechanics with the aim of improving prediction of the stresses and strains experienced by fossil crania as they deform during biting (Ledogar, et al., 2016, Smith, et al., 2015b, Strait, et al., 2010, Strait, et al., 2009, Wroe, et al., 2010). Sensitivity studies are of particular relevance here as validation is not possible for fossils. FEA applied to fossils has become popular (Cox, et al., 2011, Cox, et al., 2012, Rayfield, 2007, Strait, et al., 2013, Strait, et al., 2010, Strait, et al., 2007, Strait, et al., 2009, Wroe, et al., 2010, Wroe, et al., 2007) and models are frequently based on medical CT scans. However, another challenge of fossils arises because they are often fragmented and invaded by sedimentary matrix that, due to mineralization processes, is undistinguishable, or at least very difficult to distinguish, from bone in scans. This often precludes, for example, segmentation of sedimentary matrix from

bone and does not allow fossils to be modelled reliably in terms of their full anatomical complexity. Indeed, given the multiscale organisation of bone, teeth and soft tissues, it is not within the reach of present technology to produce an accurately realistic model. Moreover, increasing model complexity demands higher computational power for solution (Groning, et al., 2012).

Model simplification in geometry is therefore useful and necessary to overcome these limitations (Fitton, et al., 2015). Assessment of the impact of simplifications typically relies on comparison of variables of interest in subsequent FEA. Thus, researchers commonly focus on stress/strain magnitudes and directions and compare how different modelling decisions impact on those variables (Groning, et al., 2012, Reed, et al., 2011, Strait, et al., 2005, Szwedowski, et al., 2011, Wood, et al., 2011), although bite force has also been used to assess model sensitivity (Fitton, et al., 2012, Sellers and Crompton, 2004). Beyond this, the methods of geometric morphometrics have recently been applied to this task; to compare the deformations of variant models and estimate the impact of such simplifications on results (Fitton, et al., 2015, Fitton, et al., 2012, Godinho, et al., 2017, Toro-Ibacache, et al., 2016).

The application of GM methods to FEA output is discussed below in more detail, as it is used for the reconstruction of fossils for FEA and in the creation of models of interesting real and hypothetical forms.

2. How GM can help in reconstruction

Once the segmentation process is finished, reconstruction of missing anatomical regions begins. This process usually combines imaging software (e.g. Avizo/Amira/Mimics/Geomagic) and GM to approximately restore the original geometry of an incomplete or distorted specimen (Weber, 2015, Weber and Bookstein, 2011). In specimens that preserve one side intact, the most straightforward approach is to use bilateral symmetry (Gunz, et al., 2009). In such cases it is possible to reflect the preserved regions onto the incomplete side and use them to replace the missing areas (Gunz, et al., 2009). However, no skeletal structures are completely symmetric and they present different magnitudes of asymmetry (Quinto-Sánchez, et al., 2015). Thus, reflected regions will not perfectly fit the remaining preserved anatomy. To overcome this mismatch, and account for asymmetry, it is possible to use the thin plate spline (TPS) function to warp the reflected

structure onto the remaining preserved anatomy (Gunz, et al., 2009). Even though this is a desirable approach, fossils often lack preserved structures on both sides or along the midline, thus precluding reflection. In these cases reference based reconstruction (Gunz, et al., 2004, Gunz, et al., 2009) should be used. The choice of reference specimen should be considered carefully so as to not bias the reconstruction and it has been suggested that references should be species specific (Gunz, et al., 2009, Senck, et al., 2015, Zollikofer and Ponce de León, 2005). Such reconstructions may be statistical or geometric (Gunz, et al., 2004, Gunz, et al., 2009, Neeser, et al., 2009). Statistical reconstruction uses covariances among landmarks in a given sample to predict the location of missing landmarks via multivariate regression (Gunz, et al., 2009, Neeser, et al., 2009). Geometric reconstruction uses the TPS function to estimate the position of the missing landmarks based on known ones (Gunz, et al., 2004, Gunz, et al., 2009). The latter has the advantage of requiring one single specimen, which may be a particular individual or a mean specimen calculated from a given sample using GM (Gunz, et al., 2009) but omits information on intra specific covariations. However, Senck and Coquerelle (2015) show that using mean specimens yields good results when reconstructing large portions of incomplete specimens. Further where sample sizes are limited to one or a few specimens, as with fossils, TPS based warping can be applied, whereas statistical approaches cannot.

3. How GM can generate interesting hypothetical forms

Transforming an existing model into a target specimen is of significant value in allowing us to visualise the results of GM analyses. To that end an original specimen may be landmarked densely and then warped into a target that was landmarked similarly (O'Higgins, et al., 2011, Stayton, 2009). Models that represent extremes of morphological variation within a taxon may be created applying a similar approach. Such models can readily be used to simulate mechanical loading and examine the impact of intra-specific morphological variance on mechanical function (Smith, et al., 2015a). One major obstacle to using such an approach is that accurate warping of one specimen into another requires many landmarks and semilandmarks and even then, internal structures such as tooth roots, sinuses and cancellous bone are unlikely to be warped to the form they would have in the target specimen. This is because such internal architecture is very finely detailed and sinuses and cancellous bone architecture are, to great extent, the result of adaptation in the specific individual to habitual loading, this is not accounted for by warping alone. Any errors in warping will therefore

likely impact the resulting deformations of the FE model. An alternative is to warp ‘solid’ models, ones in which all that is represented is the geometry of the cranial surfaces with the spaces in between infilled with homogenous material. Cancellous bone and sinuses are filled and teeth are not represented as distinct structures, but merely as material with the properties of bone, and with roots merged with the surrounding bone. This is a drastic manoeuvre and a gross simplification. As such, the question arises as to what solid simplified models can tell us?

Parr et al. (2012) examined the impact of infilling mandibular cavities on the deformations (bending displacements and strain magnitudes frequency) experienced by the mandible of a varanoid lizard during simulated loading. They show that models with infilled cavities deform less than, but generally similarly to, models with preserved cavities. Likewise, Fitton et al. (2015) investigated the effects of simplifying details of internal anatomy (presence/absence of the maxillary sinus) and material properties of teeth in a *Macaca fascicularis* cranium, concluding that it does not impact significantly on large scale deformations but it does have localized effects in strain distributions. Toro-Ibacache (2016) addressed the impact of segmentation protocols and of simplifying material properties of a cadaveric human cranium. They concluded that segmentation protocols can have a significant impact on large scale deformations but that simplifying material properties (differentiating trabecular bone from cortical bone vs not differentiating between the two) had little impact on mode of deformation. Thus, if constraints and loads are held constant, solid models behave similarly to much more detailed ones. The key difference emerging from these studies is that the solid models deform less, and so absolute magnitudes of deformation (measured as strains or in terms of changes in size and shape; see below) are not accurately predicted while the mode of deformation (how it deforms) is more consistent. This leads to the realisation that solid models are useful in studies where absolute magnitudes of strains are of no interest but rather, the focus is on mode, how a cranium deforms.

These findings open up the possibility of carrying out many interesting ‘virtual experiments’ by warping or modifying skeletal anatomy to predict the functional role of particular features (O’Higgins, et al., 2011). Strait et al. (2007) applied this virtual experiment approach to infer the relevance of thick palates in Australopiths by experimentally thickening the hard palate of a *Macaca fascicularis* and measure resulting strains. Fitton et al. (2009) reconstructed a specimen of *Australopithecus africanus* (STS 5) and warped the zygomatic region to that of a

Paranthropus boisei (OH 5) while maintaining the remaining anatomy constant. In both cases, the impact of such modifications was assessed in terms of their impact on stresses and strains in the face.

4. How GM can be used to compare FEA results

While stresses and strains from FEA are informative with regard to how skeletal structures bear loads and where they are likely to fail at a localized level (elements or nodes of elements) they do not allow ready assessment of how the model deforms as a whole, for instance, how it bends, twists and undergoes other changes in size and shape. Rather, such modes have to be inferred from strain contour maps based on expertise and knowledge.

GM, on the other hand, uses configurations of landmark coordinates and multivariate statistics to assess how specimens differ in form, thereby quantifying morphological differences in size and shape. Thus, it has been proposed that GM can be used to measure and describe global deformations (defined here as changes in size and shape) of models under loading (O'Higgins, et al., 2011, O'Higgins, et al., 2012). This approach differs from GM shape analyses in that size is also simultaneously considered, because loadings change the shape and the size of objects. The basis and application of this approach is described more fully in section 5.3.

5. Example Studies

To illustrate how the approaches described above are applied in practice, example studies are presented and reviewed, below.

5.1 Reconstruction of crania

We illustrate the application of GM to reconstruction using a CT scan of the cranium of Kabwe 1, which is remarkably well preserved but still presents missing and damaged anatomy due to taphonomic and pathological processes (Schwartz and Tattersall, 2003). Missing anatomical regions include a large portion of the right side of the cranial vault and base (affecting parts of the right temporal, parietal, zygomatic and occipital bone), a small region of the alveolus of the maxilla, teeth and small portions of the orbital cavities (Figure 1A). The reconstruction was based on a CT scan (courtesy of Robert Kruszynski, Natural

History Museum, London) performed using a Siemens Somatom Plus 4 CT scanner, with voxel size of 0.47 x 0.47 x 0.50 mm and 140 kVp. Reconstruction started with the segmentation of the existing anatomy from the volume. Reconstruction of the left side of the vault followed, and this was later used to restore the large region missing from the right side of the cranium. Lastly, all remaining missing anatomical regions were reconstructed. Segmentation was performed in Avizo 7.0 (Visualization Sciences Group Inc.) and used a variety of approaches. The initial segmentation applied a half maximum height value (HMHV; Spoor et al., 1993) to the whole volume to threshold segment it. Regional thresholds were subsequently calculated and applied to specific anatomical regions as a second step because the HMHV did not segment thin bones. Manual segmentation was also applied for fine details of thin bones that were not picked up by the two previous approaches. Because teeth present clearly different grey values specific thresholds were calculated and applied so as to not overestimate their dimensions. Last, existing sedimentary matrix was removed manually.

Once the segmentation of existing structures was complete, the large missing region of the right half of the cranium was restored by reflecting the existing contralateral half and fitting (warping) it to the existing structures. This last step used the TPS function and is necessary because crania are not absolutely symmetric. This warping is achieved by placing matching landmarks on the damaged region and reflected fragment and then deforming (warping) the fragment to the cranium using the 'Bookstein' warping function. This resulted in an almost perfect fit between the restored and preserved anatomy, requiring only minimal manual editing. Restoration of the damaged alveolar process of the right hemi-maxilla was also achieved by reflecting the preserved left region. Existing gaps (such as the one present in the orbital surfaces of the maxilla and ethmoid, internal nasal walls, maxilla, occipital bone, left temporal bone, ethmoid bone and vomer) were restored using a combination of manual editing and the software Geomagic Studio 2011 (courtesy of DR W. Sellers, University of Manchester) to interpolate between existing bone edges. The missing posterior region of the occipital bone was reconstructed using the occipital of a modern human cranium, which was manually edited using Geomagic to adjust its morphology. Teeth were preferentially restored by reflecting existing antimeres. When this was not possible portions of teeth from a modern human were used to reconstruct incomplete teeth (final result of reconstruction in Figure 1B).

Figure 1

5.2 Hypothetical forms

FEA may be applied to any model, whether it represents a real specimen or not. For instance a prior GM analysis may have established the mean form and limits of variation of a landmark configuration taken on a sample of crania. Rather than be interested in how any particular specimens perform, we may be interested in the range of performances represented by the sample. Earlier we noted that solid models, in which internal detail is grossly simplified and filled, provide a reasonable basis for experimental manipulation of FE models to assess specific questions such as the effects of varying palatal thickness or maxillary morphology. This same principle can be extended to whole landmark configurations such as those representing the limits of variation of a sample. By using triplets of thin plate splines to warp whole crania between the mean and these limits of variation hypothetical crania can be created. They do not represent real crania but rather a statistical result from prior morphometric analyses, in this case limits of variation but also, feasibly, through regression or partial least squares (PLS), they could represent forms at the limits of cranial covariation with some interesting ecological or functional variables (e.g. climatic or dietary data, measured bite forces etc.). FEA is then carried out on these hypothetical forms to see how the modes of variation of cranial form identified in the analysis impact performance when the cranium is loaded.

This warping approach is illustrated here using a simple example; the Kabwe 1 cranium warped into a mean Neanderthal (model 2) using thin plate splines based on classical and sliding semi-landmarks. Classical landmarks (Figure 2, red spheres) of the mean Neanderthal were calculated from 4 Neanderthal crania (Gibraltar 1, Guattari, La Chapelle-aux-Saints, La Ferrassie). The sliding semi-landmarks on the maxilla and brow-ridge (yellow spheres) were calculated from the 4 specimens and the sliding semi-landmarks of the vault and zygoma (light blue spheres) were calculated from the 2 crania in which these structures are almost completely preserved (Guattari and La Ferrassie). In Figure 2, the original model of Kabwe is shown on the left (Figure 2A) and the warped ‘mean Neanderthal’ on the right (Figure 2B). It is clear that a visually satisfactory result is obtained but of course internal architecture (tooth

roots, cortical thicknesses, cavities, sinuses and cancellous bone) will also be warped, not necessarily in such a way that they reasonably represent the average form in Neanderthals. However, by using ‘solid’ models as described above such errors are avoided. The FEA in such a circumstance does not aim to predict and compare actual deformations but rather it provides an answer to a different type of question: how do the differences in external form between these models impact mode and magnitude of deformation? This approach is more limited than we may wish but it is useful in many contexts, for instance in considering how facial retraction vs projection, or brachycephaly vs dolichocephaly, or the mode of form variation predicted by e.g. climate or diet etc. impact on model performance. These are more general questions whose answer does not rest on study of single specimens, but rather on consideration of general modes of variation and their general effects.

Figure 2

5.3 Application of GM methods to the comparison of FEA results

As noted earlier a third way in which GM methods complement FEA is through comparison of deformations that occur due to loading (O'Higgins, et al., 2011, O'Higgins, et al., 2012). This approach has been applied in several studies (Cox, et al., 2011, Fitton, et al., 2015, Groning, et al., 2012, Groning, et al., 2011a, Holland, 2013, Prôa, 2013, Toro-Ibacache, et al., 2016). Such analyses of deformation rely on assessment of changes in model size and shape, rather than of shape alone as is common in GM studies of organismal variation. This is because as a model is loaded it changes in both size and shape, and it makes no sense to focus on one aspect alone (shape or size). In consequence size and shape are analysed jointly, using rescaled shape coordinates from GPA. The resulting size and shape distances between unloaded and loaded forms describe the magnitudes of deformation and the direction of the vector connecting unloaded and loaded forms in the size and shape space describes the mode of deformation. These vectors can be compared among different load cases applied to the same model or among different models by ignoring the differences in size and shape among unloaded forms and focussing in the vectors connecting unloaded and loaded forms.

We illustrate the application of this approach by summarizing a study (Godinho, et al., 2017, Toro-Ibacache, et al., 2016) that examines the impact of simplifications of a cadaveric *Homo sapiens* cranium on the resulting modes of deformation predicted by FEA. Specifically, it assesses the impact of simplifications among a three materials model (cortical bone, cancellous bone and teeth; model 3), a two materials (cortical bone and teeth; model 2) and a one material model (everything with material properties of cortical bone; model 1). Thus model 1 is a simple ‘solid’ model (see above) and model 3 is a much more anatomically accurate model. The models are loaded to simulate a bite on the first molar, although the applied forces are not physiological, rather they replicate the loading of an accompanying validation study to facilitate comparison with that in ongoing work.

The results in terms of strain contour plots (not shown), suggest that variations among models generally impact on magnitudes of strains but not so much on the distribution of regions of high and low strain throughout the model. The GM analysis of deformations complements these findings. Size and shape distances are calculated by multiplying the shape coordinates (from GPA) of each specimen by that specimen’s original centroid size. This results in the specimens being represented by points in a (size and shape) space that can be thought of as the space of GPA aligned coordinates (Slice 2001), an approximation of Kendall’s shape space, with size as an additional dimension. The vector of centroid size (the additional dimension) at any point on the manifold can be visualised as passing radially from the centroid of the manifold of this space (zero size), through the manifold (centroid size = 1) and beyond to infinity (infinite size). When centroid size is 1, the objects lie on the manifold of the space of GPA aligned coordinates (Figure 3). The resulting space differs from the classic size and shape space (Dryden and Mardia, 1998) that results from translating and rotating, but not scaling landmark configurations. In particular, the rotations of configurations with respect to each other differ because size influences rotation. In consequence the estimates of mean size and shape (the size and shape variables; translated and rotated coordinates) obtained by these two approaches, the resulting covariance matrix, and so PCA, also differ. However in the application to FEA, where deformations are extremely small, the resulting size and shape differences are negligible. Either space could be used, with almost no difference in results, but the approach we adopt is useful in understanding how shape analysis and size and shape analysis are related (Figure 3). Thus, simply making the model stiffer or less stiff (material properties) or applying the same force vectors but varying their magnitudes results in greater or less deformation; the vectors connecting unloaded and loaded models simply scale directly with force or inversely with Young’s modulus (a measure of stiffness). Deformations (size

and shape distances) also scale inversely with model centroid size if loads, geometry and material properties are held constant. In contrast Procrustes distances scale inversely with the square of centroid size. Figure 3 illustrates these scaling relationships with centroid size. Thus if we take the shape of the black point (a; on the GPA hemisphere, centroid size =1; Fig. 3) to be the unloaded form and the grey point (b) as the shape of the loaded form, the distance between them represents the deformation in shape and approximates Procrustes distance when variations are small. If size also differs due to loading, then the loaded form does not lie on the hemisphere but is above (grey point, c) or below it depending on if it increased or decreased in centroid size. The distance (a-c) between loaded and unloaded forms is the size and shape distance and is a measure of deformation (change in size and shape with loading).

If the same forces and same material properties apply but the unloaded form is larger (black point, d, on the outer semicircle representing the GPA hemisphere with centroid size >1 in Fig 3) the resulting deformation in size and shape is less (distance d-f; which in this diagram is shown larger than in reality to facilitate visualisation). The physics dictate that the size and shape distances (deformations) between unloaded and loaded objects scale inversely with centroid sizes of the unloaded objects; bigger forms deform less under the same load. However, shape change due to loading (Procrustes distance as opposed to size and shape distance) scales inversely with the *square* of the centroid size of the unloaded object. Thus, scaling the unloaded large object, d, to centroid size 1, results in it overlying point a, the unloaded object with centroid size 1 (these are identical in shape but differ only in size). Scaling the loaded large object, f, to centroid size 1 projects it along a radius (dashed line in Fig. 3) through point e to an intersection, g, with the arc of the GPA hemisphere. As a result of this scaling, the ratio of Procrustes distances (a-b)/(a-g) is the inverse of the ratio of the squares of centroid sizes of the unloaded forms, a and d.

These scaling ratios are important because they allow us to account (at least approximately) for differences in size when comparing deformations predicted by FEA among similar objects using geometric morphometric methods. Such scaling is inevitably an approximation unless the objects whose deformations are being compared are the same shape, differing only in size. As shapes become more different, it makes less sense to compare deformations and the degree of approximation in scaling increases.

Figure 3

Principal components analysis using the covariance matrix among size and shape variables can be used to visualise and compare deformations. Figure 4 presents the first two principal components from the sensitivity study we conducted on a *Homo sapiens* of model simplification with regard to segmentation and allocation of material properties. These account for some 99% of the total variance and so fairly represent the results. Included in the analysis are the unloaded model and the three variants of model segmentation (model 1, whole model as cortical bone = 17 GPa; model 2, bone = 17 GPa and teeth = 50 GPa; model 3, cortical bone = 17GPa, cancellous bone = 56 MPa, teeth = 50 GPa; all materials allocated a Poisson's ratio of 0.3) after loading in a simulated first molar bite. Model 3 is also loaded in a simulated incisor bite. This allows the effects of simplification to be compared against the effect of varying bite point. The molar bites cluster away from the incisor bite, indicating they are more similar in mode of deformation. The modes of variation are represented by the vectors connecting unloaded and loaded models. They are visualised by the inset warped surface models and transformation grids, computed using thin plate splines and magnified 500 times to facilitate interpretation. Models 2 and 1 overlies each other and so are represented by a single point. This implies that representing dental roots as cortical bone has little effect. Modes of deformation differ greatly between incisor and molar bites and consist mainly of upwards deflection of the anterior maxilla in the former and of the lateral maxilla in the latter. With regard to the molar bites, simplification has its greatest impact when cancellous bone is allocated the material properties of cortical, effectively making a 'solid' model. The effect is to reduce the degree of deformation as is reflected in the shorter vector connecting models 1 and 2 with the unloaded than that connecting model 3. Similarly the degree of deformation evident in the inset warpings is reduced. There is a difference in mode of deformation as evidenced by the angle between these vectors but the difference in mode is less obvious in comparing the inset warping for models 2 and 3 with that for model 1.

The impact of simplification on mode of deformation is small compared to the large difference between molar and incisor bites.

Figure 4

This simple analysis can be extended to more complex and interesting questions concerning multiple variants of models and to the comparison of deformations among models (O'Higgins and Milne, 2013) by focusing on differences among vectors of deformation rather than differences among unloaded forms. This application of GM is particularly useful in relation to FEA sensitivity studies providing an easily visible and quantifiable approach to the assessment of model "error" and sensitivity. Comparisons can be made within and between models to assess whether differences in performance due to modelling assumptions are drowning out any meaningful biological signals.

6. Discussion

The last three decades have seen an explosion of advances in techniques pertinent to the study of skeletal change through time. Morphometrics underwent a revolution (Adams, et al., 2004, Rohlf and Marcus, 1993) beginning in the late 1970's (Bookstein, 1978) and gathering pace through the next three decades. This, in common with the tools for high resolution imaging, visualisation and manipulation of images, took great advantage of the advances in computing that occurred over the same period. These same advances in computational power led to the development of increasingly sophisticated software tools for FEA, to simulate and predict the effects of loadings on structures.

All of these tools are in common use today in the field of Archaeology, in particular they have been driven by work on fossil material, but increasingly they are applied to more recent skeletal finds, archaeobotany (García-Granero, et al., 2016, Ros, et al., 2014), zooarchaeology (Cucchi, et al., 2011, Evin, et al., 2013, Owen, et al., 2014) and to material culture such as ancient architecture (Levy and Dawson, 2009), stone tools (Buchanan and Collard, 2010, Buchanan, et al., 2011, Okumura and Araujo, 2014), and pottery (Hein, et al., 2008, Kilikoglou and Vekinis, 2002, Wilczek, et al., 2014). As these tools have become more commonly applied, useful ways of combining them have come to the fore. Thus, GM methods combined with tools for imaging and image manipulation can play an important role in the reconstruction of skeletal material, as illustrated by the first example we present in this paper.

Reconstruction provides data for morphometric analyses and GM has proven powerful in this domain. Beyond the fact that these methods provide approaches that are statistically robust and well understood, GM's great advantage for many workers lies in the ability to visualise the results of statistical analyses as warpings of the mean form. These visualisations close the loop between measurement, statistics and interpretation of results in terms of changes in size and shape. They also can be used to produce 3D models of the results of statistical analyses such as mean forms or forms representing extremes of variation or extremes of interesting modes of variation, such as the limits of regressions of form on ecological, behavioural and functional data. In turn, such forms are potentially interesting targets for FEA. For instance, the results of a study of how cranial form covaries with the toughness of diet might be actualised as a pair of 3D surfaces representing crania at the limits of the regression; those suited to tough and those suited to less tough diets. These can be submitted to FEA to explore how each responds to loading and, in this way, link modes of morphological variation to load resistance. This kind of analysis provides a very direct way of exploring how form and function interact.

These kinds of studies depend critically on the validity of FEA modelling and on how sensitive such modelling is to errors in model building and loading. Validity is assessed by comparing predicted strains with directly measured, real strains. Sensitivity, on the other hand is assessed by varying model parameters to replicate likely errors and comparing results among (often many) variant models as in the example we provide earlier. In this endeavour, GM has been usefully combined with FEA.

Size and shape analysis allows ready understanding of the effects of different model building decisions in terms of how the models deform and how they differ in deformation. It leads to statements about changes in form such as how a skull twists or bends under loading. If, instead of landmarks the coordinates of all nodes of the finite element mesh are submitted to analysis, strains can be computed from the coordinates of the unloaded and loaded meshes.

On the other hand the concentrations of stresses or strains in localised regions are useful predictors of failure and while the overall distribution of strains can be used to infer global modes of deformation this requires simultaneous interpretation of one contour map for each principal strain (2 in 2D analyses and 3 in 3D). Thus the approaches can be considered complementary. GM analyses inform with regard to how loading deforms an object, in terms

of changes in size and shape. On the other hand, stresses and strains inform with regard to the likelihood of failure in particular anatomical regions and how distributions of high and low strains may eventually relate to (re)modelling fields. Each can be used to infer the other, thus GM analyses that use the coordinates of the nodes of an FE mesh result in visualisations of deformations of that mesh and strains can be computed and displayed in these meshes, while strains can be used to infer global degrees and modes of deformation. It should be noted that the metric of the GM analysis, the Procrustes size and shape distance relates to changes in size and shape, not the risk of failure. It differs from metrics derived from strains. These describe different aspects of deformation that are complementary, but not coincident, in interpreting FEA results.

Beyond sensitivity analyses, GM methods have been extended to the task of comparing deformations among different specimens modelled and loaded in equivalent ways (Milne and O'Higgins, 2012, O'Higgins and Milne, 2013). In this case the analysis focuses on differences in vectors of deformation rather than the differences between unloaded forms. This is achieved by computing deformations as differences between registered loaded and unloaded forms. They can be visualised by adding these vectors to a convenient unloaded form such as the mean of all unloaded specimens. Beyond comparisons of deformation, it is also possible to use GM approaches to assess the association between deformation under loading and other interesting factors such as skeletal form or ecological variables through regression of PLS analyses. This has not yet been much exploited in the literature but is likely to increasingly be taken up as a useful approach to the interpretation of the biological significance of differences in modes and magnitudes of variation. Differences among models in size, applied forces and material properties can be taken into account by 'correcting' the magnitudes of deformations according to the known scaling relationships described above.

The application of GM methods in conjunction with FEA is as yet in its infancy. There are clear roles for GM methods in reconstruction, the production of models with modified geometry to explore how form and function interact and in comparing the results of FEAs among models and load cases. Each of these approaches has potential benefits and pitfalls and, in time, with increasing numbers of studies applying these methods we will better understand where they are applicable and where not. At present these combined GM/FEA approaches are still fairly novel and some years of methodological development can be anticipated.

582

583 **Acknowledgements**

584 We are grateful for support provided to R. M. Godinho by the Portuguese Foundation for
585 Science and Technology (PhD funding reference: SFRH/BD/76375/2011) and to Fred
586 Bookstein, Dennis Slice, Ian Dryden and Chris Klingenberg for their feedback and critiques
587 of particularly the GM analysis of deformations resulting from FEA, provided on many
588 occasions over recent years.

589

References

- Adams, D.C., Rohlf, F.J., Slice, D.E., 2004. Geometric morphometrics: ten years of progress following the ‘revolution’, *Italian Journal of Zoology* 71, 5-16.
- Antón, S.C., 1990. Neandertals and the anterior dental loading hypothesis: a biomechanical evaluation of bite force production, *Kroeber Anthropological Society Papers* 71-72, 67-76.
- Attard, M.R.G., Parr, W.C.H., Wilson, L.A.B., Archer, M., Hand, S.J., Rogers, T.L., Wroe, S., 2014. Virtual Reconstruction and Prey Size Preference in the Mid Cenozoic Thylacinid, *Nimbacinus dicksoni* (Thylacinidae, Marsupialia), *Plos One* 9, e93088.
- Bates, K.T., Falkingham, P.L., 2012. Estimating maximum bite performance in *Tyrannosaurus rex* using multi-body dynamics, *Biol Letters* 8, 660-664.
- Bookstein, F., 1978. *The Measurement of Biological Shape and Shape Change*, Springer, Berlin.
- Braun, S., Bantleon, H.-P., Hnat, W.P., Freudenthaler, J.W., Marcotte, M.R., Johnson, B.E., 1995. A study of bite force, part 1: Relationship to various physical characteristics, *The Angle Orthodontist* 65, 367-372.
- Bright, J.A., Groning, F., 2011. Strain Accommodation in the Zygomatic Arch of the Pig: A Validation Study Using Digital Speckle Pattern Interferometry and Finite Element Analysis, *Journal of Morphology* 272, 1388-1398.
- Buchanan, B., Collard, M., 2010. A geometric morphometrics-based assessment of blade shape differences among Paleoindian projectile point types from western North America, *J Archaeol Sci* 37, 350-359.

612 Buchanan, B., Collard, M., Hamilton, M.J., O'Brien, M.J., 2011. Points and prey: a
 613 quantitative test of the hypothesis that prey size influences early Paleoindian projectile point
 614 form, *J Archaeol Sci* 38, 852-864.

615 Cox, P.G., Fagan, M.J., Rayfield, E.J., Jeffery, N., 2011. Finite element modelling of squirrel,
 616 guinea pig and rat skulls: using geometric morphometrics to assess sensitivity, *J Anat* 219,
 617 696-709.

618 Cox, P.G., Rayfield, E.J., Fagan, M.J., Herrel, A., Pataky, T.C., Jeffery, N., 2012. Functional
 619 Evolution of the Feeding System in Rodents, *Plos One* 7.

620 Cox, P.G., Rinderknecht, A., Blanco, R.E., 2015. Predicting bite force and cranial
 621 biomechanics in the largest fossil rodent using finite element analysis, *J Anat* 226, 215-223.

622 Cucchi, T., Hulme-Beaman, A., Yuan, J., Dobney, K., 2011. Early Neolithic pig
 623 domestication at Jiahu, Henan Province, China: clues from molar shape analyses using
 624 geometric morphometric approaches, *J Archaeol Sci* 38, 11-22.

625 Curtis, N., Kupczik, K., O'Higgins, P., Moazen, M., Fagan, M., 2008. Predicting skull
 626 loading: Applying multibody dynamics analysis to a macaque skull, *Anat Rec* 291, 491-501.

627 Degrange, F.J., Tambussi, C.P., Moreno, K., Witmer, L.M., Wroe, S., 2010. Mechanical
 628 Analysis of Feeding Behavior in the Extinct "Terror Bird" *Andalgalornis steulleti*
 629 (Gruiformes: Phorusrhacidae), *Plos One* 5, e11856.

630 Demes, B., 1987. Another Look at an Old Face - Biomechanics of the Neandertal Facial
 631 Skeleton Reconsidered, *J Hum Evol* 16, 297-303.

632 Demes, B., Creel, N., 1988. Bite Force, Diet, and Cranial Morphology of Fossil Hominids, *J*
 633 *Hum Evol* 17, 657-670.

634 Dryden, I.L., Mardia, K.V., 1998. Statistical Shape Analysis, Wiley-Blackwell.

635 Eng, C.M., Lieberman, D.E., Zink, K.D., Peters, M.A., 2013. Bite force and occlusal stress
636 production in hominin evolution, *Am J Phys Anthropol* 151, 544-557.

637 Evin, A., Cucchi, T., Cardini, A., Strand Vidarsdottir, U., Larson, G., Dobney, K., 2013. The
638 long and winding road: identifying pig domestication through molar size and shape, *J*
639 *Archaeol Sci* 40, 735-743.

640 Fitton, L., Groening, F., Cobb, S., Fagan, M., O'Higgins, P., 2009. Biomechanical
641 Significance of Morphological Variation between the Gracile *Australopithecus Africanus*
642 (STS5) and Robust *Australopithecus Boisei* (OH5), *J Vertebr Paleontol* 29, 96a-96a.

643 Fitton, L.C., Prôa, M., Rowland, C., Toro-Ibacache, V., O'Higgins, P., 2015. The Impact of
644 Simplifications on the Performance of a Finite Element Model of a *Macaca fascicularis*
645 Cranium, *The Anatomical Record* 298, 107-121.

646 Fitton, L.C., Shi, J.F., Fagan, M.J., O'Higgins, P., 2012. Masticatory loadings and cranial
647 deformation in *Macaca fascicularis*: a finite element analysis sensitivity study, *J Anat* 221,
648 55-68.

649 Gans, C., de Vree, F., 1987. Functional bases of fiber length and angulation in muscle,
650 *Journal of Morphology* 192, 63-85.

651 García-Granero, J.J., Arias-Martorell, J., Madella, M., Lancelotti, C., 2016. Geometric
652 morphometric analysis of *Setaria italica* (L.) P. Beauv. (foxtail millet) and *Brachiaria ramosa*
653 (L.) Stapf. (browntop millet) and its implications for understanding the biogeography of small
654 millets, *Vegetation History and Archaeobotany* 25, 303-310.

655 Godinho, R.M., O'Higgins, P., 2017. Virtual reconstruction of cranial remains: the H.
656 Heidelbergensis, Kabwe 1 fossil, in: Thompson, T., Errickson, D. (Eds.), *Human remains -*
657 *Another dimension: the application of 3D imaging in funerary context*, Elsevier, London, pp.
658 135-147.

659 Godinho, R.M., Toro-Ibacache, V., Fitton, L.C., O'Higgins, P., 2017. Finite element analysis
660 of the cranium: Validity, sensitivity and future directions, *Cr Palevol* 16, 600-612.

661 Groning, F., Fagan, M., O'Higgins, P., 2012. Modeling the Human Mandible Under
662 Masticatory Loads: Which Input Variables are Important?, *Anat Rec* 295, 853-863.

663 Groning, F., Fagan, M.J., O'Higgins, P., 2011a. The effects of the periodontal ligament on
664 mandibular stiffness: a study combining finite element analysis and geometric
665 morphometrics, *J Biomech* 44, 1304-1312.

666 Groning, F., Liu, J., Fagan, M.J., O'Higgins, P., 2009. Validating a voxel-based finite element
667 model of a human mandible using digital speckle pattern interferometry, *J Biomech* 42, 1224-
668 1229.

669 Groning, F., Liu, J., Fagan, M.J., O'Higgins, P., 2011b. Why Do Humans Have Chins?
670 Testing the Mechanical Significance of Modern Human Symphyseal Morphology With Finite
671 Element Analysis, *Am J Phys Anthropol* 144, 593-606.

672 Gunz, P., Mitteroecker, P., Bookstein, F., Weber, G., 2004. Computer-aided reconstruction of
673 incomplete human crania using statistical and geometrical estimation methods, *Computer*
674 *Applications and Quantitative Methods in Archaeology*, Archaeopress, pp. 92–94.

675 Gunz, P., Mitteroecker, P., Neubauer, S., Weber, G.W., Bookstein, F.L., 2009. Principles for
676 the virtual reconstruction of hominin crania, *J Hum Evol* 57, 48-62.

677 Hein, A., Georgopoulou, V., Nodarou, E., Kilikoglou, V., 2008. Koan amphorae from
678 Halasarna – investigations in a Hellenistic amphora production centre, *J Archaeol Sci* 35,
679 1049-1061.

680 Holland, M., 2013. The effect of the inclusion of the periodontal ligament upon the stiffness
681 of a human cranial finite element model: a validated sensitivity study, HYMS, University of
682 York, York.

683 Josephson, R.K., 1975. Extensive and intensive factors determining the performance of
684 striated muscle, *J Exp Zool* 194, 135-153.

685 Kikuchi, M., Koriath, T.W.P., Hannam, A.G., 1997. The Association Among Occlusal
686 Contacts, Clenching Effort, and Bite Force Distribution in Man, *J Dent Res* 76, 1316-1325.

687 Kilikoglou, V., Vekinis, G., 2002. Failure Prediction and Function Determination of
688 Archaeological Pottery by Finite Element Analysis, *J Archaeol Sci* 29, 1317-1325.

689 Kupczik, K., Dobson, C.A., Fagan, M.J., Crompton, R.H., Oxnard, C.E., O'Higgins, P., 2007.
690 Assessing mechanical function of the zygomatic region in macaques: validation and
691 sensitivity testing of finite element models, *J Anat* 210, 41-53.

692 Ledogar, J.A., Smith, A.L., Benazzi, S., Weber, G.W., Spencer, M.A., Carlson, K.B.,
693 McNulty, K.P., Dechow, P.C., Grosse, I.R., Ross, C.F., Richmond, B.G., Wright, B.W.,
694 Wang, Q., Byron, C., Carlson, K.J., de Ruiter, D.J., Berger, L.R., Tamvada, K., Pryor, L.C.,
695 Berthaume, M.A., Strait, D.S., 2016. Mechanical evidence that *Australopithecus sediba* was
696 limited in its ability to eat hard foods, *Nat Commun* 7.

697 Levy, R., Dawson, P., 2009. Using finite element methods to analyze ancient architecture: an
698 example from the North American Arctic, *J Archaeol Sci* 36, 2298-2307.

699 Lieberman, D., 2011. *The Evolution of the Human Head*, Harvard University Press,
700 Cambridge.

701 McCormack, S.W., Witzel, U., Watson, P.J., Fagan, M.J., Gröning, F., 2014. The
702 Biomechanical Function of Periodontal Ligament Fibres in Orthodontic Tooth Movement,
703 *Plos One* 9, e102387.

704 Milne, N., O'Higgins, P., 2012. Scaling of form and function in the xenarthran femur: a 100-
705 fold increase in body mass is mitigated by repositioning of the third trochanter, *P Roy Soc B-*
706 *Biol Sci* 279, 3449-3456.

707 Neeser, R., Ackermann, R.R., Gain, J., 2009. Comparing the accuracy and precision of three
708 techniques used for estimating missing landmarks when reconstructing fossil hominin crania,
709 *Am J Phys Anthropol* 140, 1-18.

710 O'Connor, C.F., Franciscus, R.G., Holton, N.E., 2005. Bite force production capability and
711 efficiency in neandertals and modern humans, *Am J Phys Anthropol* 127, 129-151.

712 O'Higgins, P., Cobb, S.N., Fitton, L.C., Groning, F., Phillips, R., Liu, J., Fagan, M.J., 2011.
713 Combining geometric morphometrics and functional simulation: an emerging toolkit for
714 virtual functional analyses, *J Anat* 218, 3-15.

715 O'Higgins, P., Fitton, L.C., Phillips, R., Shi, J.F., Liu, J., Groning, F., Cobb, S.N., Fagan,
716 M.J., 2012. Virtual Functional Morphology: Novel Approaches to the Study of Craniofacial
717 Form and Function, *Evol Biol* 39, 521-535.

718 O'Higgins, P., Milne, N., 2013. Applying geometric morphometrics to compare changes in
719 size and shape arising from finite elements analyses, *Hystrix, the Italian Journal of*
720 *Mammalogy* 24, 7.

721 Okumura, M., Araujo, A.G.M., 2014. Long-term cultural stability in hunter-gatherers: a case
722 study using traditional and geometric morphometric analysis of lithic stemmed bifacial points
723 from Southern Brazil, *J Archaeol Sci* 45, 59-71.

724 Oldfield, C.C., McHenry, C.R., Clausen, P.D., Chamoli, U., Parr, W.C.H., Stynder, D.D.,
725 Wroe, S., 2012. Finite element analysis of ursid cranial mechanics and the prediction of
726 feeding behaviour in the extinct giant *Agriotherium africanum*, *J Zool* 286, 171-171.

727 Owen, J., Dobney, K., Evin, A., Cucchi, T., Larson, G., Strand Vidarsdottir, U., 2014. The
728 zooarchaeological application of quantifying cranial shape differences in wild boar and
729 domestic pigs (*Sus scrofa*) using 3D geometric morphometrics, *J Archaeol Sci* 43, 159-167.

730 Paphangkorakit, J., Osborn, J.W., 1997. Effect of Jaw Opening on the Direction and
731 Magnitude of Human Incisal Bite Forces, *J Dent Res* 76, 561-567.

732 Parr, W.C.H., Chamoli, U., Jones, A., Walsh, W.R., Wroe, S., 2013. Finite element micro-
733 modelling of a human ankle bone reveals the importance of the trabecular network to
734 mechanical performance: New methods for the generation and comparison of 3D models, *J*
735 *Biomech* 46, 200-205.

736 Parr, W.C.H., Wroe, S., Chamoli, U., Richards, H.S., McCurry, M.R., Clausen, P.D.,
737 McHenry, C., 2012. Toward integration of geometric morphometrics and computational
738 biomechanics: New methods for 3D virtual reconstruction and quantitative analysis of Finite
739 Element Models, *J Theor Biol* 301, 1-14.

740 Prôa, M., 2013. Cranial Form Evolution and Functional Adaptations to Diet among
741 Papionins: A Comparative Study combining Quantitative Genetics, Geometric
742 Morphometrics, and Finite Element Analysis, Hull York Medical School, University of York,
743 York.

744 Quinto-Sánchez, M., Adhikari, K., Acuña-Alonzo, V., Cintas, C., Silva de Cerqueira, C.C.,
745 Ramallo, V., Castillo, L., Farrera, A., Jaramillo, C., Arias, W., Fuentes, M., Everardo, P., de
746 Avila, F., Gomez-Valdés, J., Hünemeier, T., Gibbon, S., Gallo, C., Poletti, G., Rosique, J.,
747 Bortolini, M.C., Canizales-Quinteros, S., Rothhammer, F., Bedoya, G., Ruiz-Linares, A.,
748 González-José, R., 2015. Facial asymmetry and genetic ancestry in Latin American admixed
749 populations, *Am J Phys Anthropol*, n/a-n/a.

750 Rak, Y., 1983. The Australopithecine Face, in: Rak, Y. (Ed.), *The Australopithecine Face*,
751 Academic Press, p. 1.

752 Rak, Y., 1986. The Neanderthal - a New Look at an Old Face, *J Hum Evol* 15, 151-164.

753 Rayfield, E.J., 2005. Aspects of comparative cranial mechanics in the theropod dinosaurs
754 *Coelophysis*, *Allosaurus* and *Tyrannosaurus*, *Zool J Linn Soc-Lond* 144, 309-316.

755 Rayfield, E.J., 2007. Finite element analysis and understanding the biomechanics and
756 evolution of living and fossil organisms, *Annu Rev Earth Pl Sc* 35, 541-576.

757 Rayfield, E.J., Norman, D.B., Horner, C.C., Horner, J.R., Smith, P.M., Thomason, J.J.,
758 Upchurch, P., 2001. Cranial design and function in a large theropod dinosaur, *Nature* 409,
759 1033-1037.

760 Reed, D.A., Porro, L.B., Iriarte-Diaz, J., Lemberg, J.B., Holliday, C.M., Anapol, F., Ross,
761 C.F., 2011. The impact of bone and suture material properties on mandibular function in
762 Alligator mississippiensis: testing theoretical phenotypes with finite element analysis, *J Anat*
763 218, 59-74.

764 Rohlf, F.J., Marcus, L.F., 1993. A revolution in morphometrics, *Trends Ecol Evol* 8, 129-
765 132.

766 Ros, J., Evin, A., Bouby, L., Ruas, M.-P., 2014. Geometric morphometric analysis of grain
767 shape and the identification of two-rowed barley (*Hordeum vulgare* subsp. *distichum* L.) in
768 southern France, *J Archaeol Sci* 41, 568-575.

769 Ross, C.F., 2005. Finite element analysis in vertebrate biomechanics, *Anat Rec Part A* 283A,
770 253-258.

771 Schwartz, J.H., Tattersall, I., 2003. *The Human Fossil Record - Craniodental Morphology of*
772 *Genus Homo*, Wiley-Liss, USA.

773 Sellers, W.I., Crompton, R.H., 2004. Using sensitivity analysis to validate the predictions of a
774 biomechanical model of bite forces, *Ann Anat* 186, 89-95.

775 Senck, S., Bookstein, F.L., Benazzi, S., Kastner, J., Weber, G.W., 2015. Virtual
776 Reconstruction of Modern and Fossil Hominoid Crania: Consequences of Reference Sample
777 Choice, *The Anatomical Record* 298, 827-841.

- 778 Senck, S., Coquerelle, M., 2015. Morphological Integration and Variation in Facial
779 Orientation in *Pongo pygmaeus pygmaeus*: A Geometric Morphometric Approach via Partial
780 Least Squares, *Int J Primatol* 36, 489-512.
- 781 Shi, J.F., Curtis, N., Fitton, L.C., O'Higgins, P., Fagan, M.J., 2012. Developing a
782 musculoskeletal model of the primate skull: Predicting muscle activations, bite force, and
783 joint reaction forces using multibody dynamics analysis and advanced optimisation methods,
784 *J Theor Biol* 310, 21-30.
- 785 Sinn, D.P., DeAssis, E.A., Throckmorton, G.S., 1996. Mandibular excursions and maximum
786 bite forces in patients with temporomandibular joint disorders, *J Oral Maxil Surg* 54, 671-
787 679.
- 788 Slice, D.E., 2001. Landmark coordinates aligned by Procrustes analysis do not lie in
789 Kendall's shape space. *Systematic biology*, 50(1), 141-149.
- 790 Slice, D.E., Chalk, J., Smith, A.L., Smith, L.C., Wood, S., Berthaume, M., Benazzi, S.,
791 Dzialo, C., Tamvada, K., Ledogar, J.A., 2013. Viewpoints: Diet and dietary adaptations in
792 early hominins: The hard food perspective, *Am J Phys Anthropol* 151, 339-355.
- 793 Smith, A.L., Benazzi, S., Ledogar, J.A., Tamvada, K., Pryor Smith, L.C., Weber, G.W.,
794 Spencer, M.A., Dechow, P.C., Grosse, I.R., Ross, C.F., Richmond, B.G., Wright, B.W.,
795 Wang, Q., Byron, C., Slice, D.E., Strait, D.S., 2015a. Biomechanical Implications of
796 Intraspecific Shape Variation in Chimpanzee Crania: Moving Toward an Integration of
797 Geometric Morphometrics and Finite Element Analysis, *The Anatomical Record* 298, 122-
798 144.
- 799 Smith, A.L., Benazzi, S., Ledogar, J.A., Tamvada, K., Pryor Smith, L.C., Weber, G.W.,
800 Spencer, M.A., Lucas, P.W., Michael, S., Shekeban, A., Al-Fadhalah, K., Almusallam, A.S.,
801 Dechow, P.C., Grosse, I.R., Ross, C.F., Madden, R.H., Richmond, B.G., Wright, B.W.,
802 Wang, Q., Byron, C., Slice, D.E., Wood, S., Dzialo, C., Berthaume, M.A., van Casteren, A.,
803 Strait, D.S., 2015b. The Feeding Biomechanics and Dietary Ecology of *Paranthropus boisei*,
804 *The Anatomical Record* 298, 145-167.

805 Stayton, C.T., 2009. Application of thin-plate-spline transformations to finite element
806 models, or, how to turn a bog turtle into a spotted turtle to analyze both, *Evolution* 63, 1348-
807 1355.

808 Strait, D.S., Constantino, P., Lucas, P.W., Richmond, B.G., Spencer, M.A., Dechow, P.C.,
809 Ross, C.F., Grosse, I.R., Wright, B.W., Wood, B.A., Weber, G.W., Wang, Q., Byron, C.,

810 Strait, D.S., Grosse, I.R., Dechow, P.C., Smith, A.L., Wang, Q., Weber, G.W., Neubauer, S.,
811 Slice, D.E., Chalk, J., Richmond, B.G., Lucas, P.W., Spencer, M.A., Schrein, C., Wright,
812 B.W., Byfton, C., Ross, C.F., 2010. The Structural Rigidity of the Cranium of
813 *Australopithecus africanus*: Implications for Diet, Dietary Adaptations, and the Allometry of
814 Feeding Biomechanics, *Anat Rec* 293, 583-593.

815 Strait, D.S., Richmond, B.G., Spencer, M.A., Ross, C.F., Dechow, P.C., Wood, B.A., 2007.
816 Masticatory biomechanics and its relevance to early hominid phylogeny: An examination of
817 palatal thickness using finite-element analysis, *J Hum Evol* 52, 585-599.

818 Strait, D.S., Wang, Q., Dechow, P.C., Ross, C.F., Richmond, B.G., Spencer, M.A., Patel,
819 B.A., 2005. Modeling elastic properties in finite element analysis: How much precision is
820 needed to produce an accurate model?, *Anat Rec Part A* 283A, 275-287.

821 Strait, D.S., Weber, G.W., Neubauer, S., Chalk, J., Richmond, B.G., Lucas, P.W., Spencer,
822 M.A., Schrein, C., Dechow, P.C., Ross, C.F., Grosse, I.R., Wright, B.W., Constantino, P.,
823 Wood, B.A., Lawn, B., Hylander, W.L., Wang, Q., Byron, C., Slice, D.E., Smith, A.L., 2009.
824 The feeding biomechanics and dietary ecology of *Australopithecus africanus*, *P Natl Acad*
825 *Sci USA* 106, 2124-2129.

826 Szwedowski, T.D., Fialkov, J., Whyne, C.M., 2011. Sensitivity analysis of a validated
827 subject-specific finite element model of the human craniofacial skeleton, *P I Mech Eng H*
828 225, 58-67.

829 Toro-Ibacache, V., Fitton, L.C., Fagan, M.J., O'Higgins, P., 2016. Validity and sensitivity of
830 a human cranial finite element model: implications for comparative studies of biting
831 performance, *J Anat* 228, 70-84.

832 Toro-Ibacache, V., Zapata Muñoz, V., O'Higgins, P., 2015. The Predictability from Skull
833 Morphology of Temporalis and Masseter Muscle Cross-Sectional Areas in Humans, *The*
834 *Anatomical Record* 298, 1261-1270.

835 Trinkaus, E., 1987. The Neandertal Face - Evolutionary and Functional Perspectives on a
836 Recent Hominid Face, *J Hum Evol* 16, 429-443.

837 Wang, Q.A., Smith, A.L., Strait, D.S., Wright, B.W., Richmond, B.G., Grosse, I.R., Byron,
838 C.D., Zapata, U., 2010. The Global Impact of Sutures Assessed in a Finite Element Model of
839 a Macaque Cranium, *Anat Rec* 293, 1477-1491.

840 Weber, G.W., 2015. Virtual Anthropology, *Am J Phys Anthropol* 156, 22-42.

841 Weber, G.W., Bookstein, F.L., 2011. Virtual Anthropology - A Guide for a New
842 Interdisciplinary Field, Springer-Verlag, Wien.

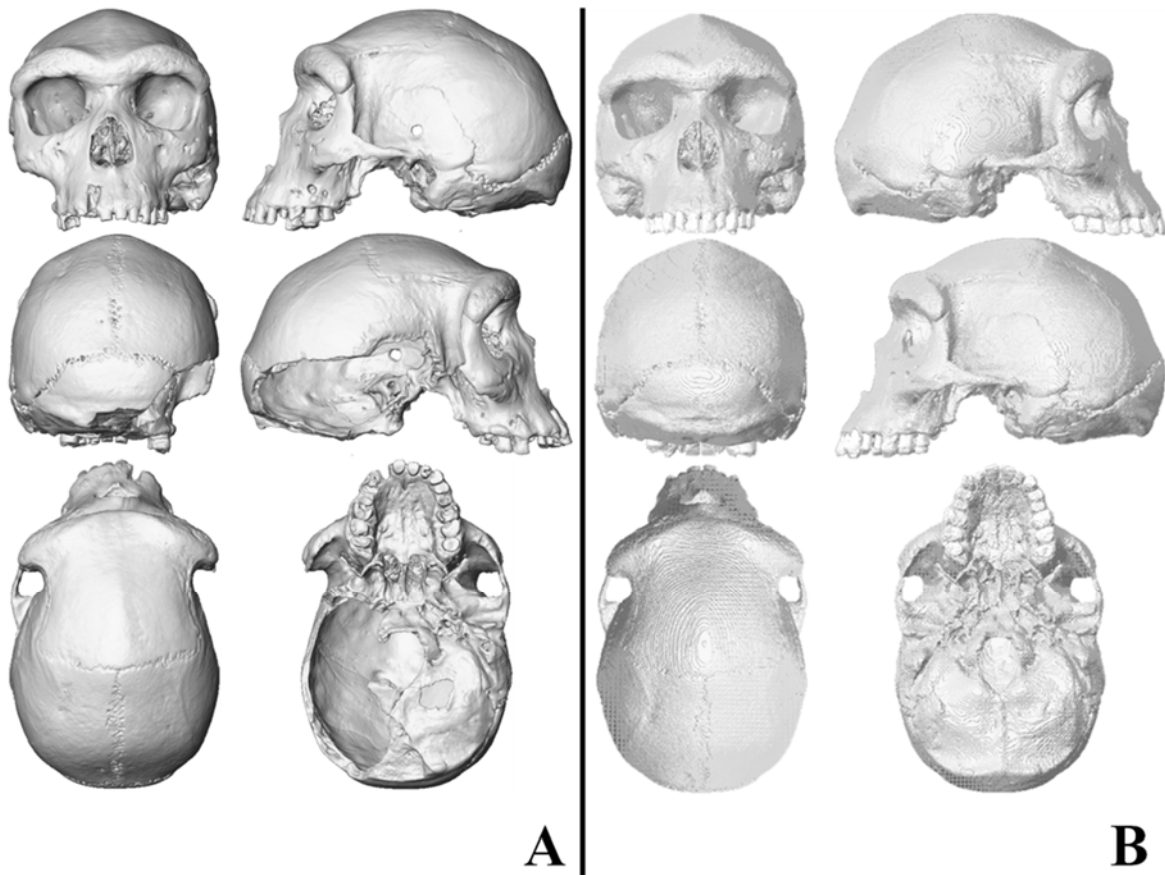
843 Weijs, W.A., 1980. Biomechanical Models and the Analysis of Form: A Study of the
844 Mammalian Masticatory Apparatus, *Am Zool* 20, 707-719.

845 Wilczek, J., Monna, F., Barral, P., Burlet, L., Chateau, C., Navarro, N., 2014. Morphometrics
846 of Second Iron Age ceramics – strengths, weaknesses, and comparison with traditional
847 typology, *J Archaeol Sci* 50, 39-50.

848 Wood, S.A., Strait, D.S., Dumont, E.R., Ross, C.F., Grosse, I.R., 2011. The effects of
849 modeling simplifications on craniofacial finite element models: The alveoli (tooth sockets)
850 and periodontal ligaments, *J Biomech* 44, 1831-1838.

- 851 Wroe, S., 2008. Cranial mechanics compared in extinct marsupial and extant African lions
852 using a finite-element approach, *J Zool* 274, 332-339.
- 853 Wroe, S., Ferrara, T.L., McHenry, C.R., Curnoe, D., Chamoli, U., 2010. The
854 craniomandibular mechanics of being human, *P Roy Soc B-Biol Sci* 277, 3579-3586.
- 855 Wroe, S., Moreno, K., Clausen, P., Mchenry, C., Curnoe, D., 2007. High-resolution three-
856 dimensional computer simulation of hominid cranial mechanics, *Anat Rec* 290, 1248-1255.
- 857 Zollikofer, C.P., Ponce de León, M.S., 2005. Virtual reconstruction: a primer in computer-
858 assisted paleontology and biomedicine, Wiley-Interscience, New Jersey.
- 859
- 860

861



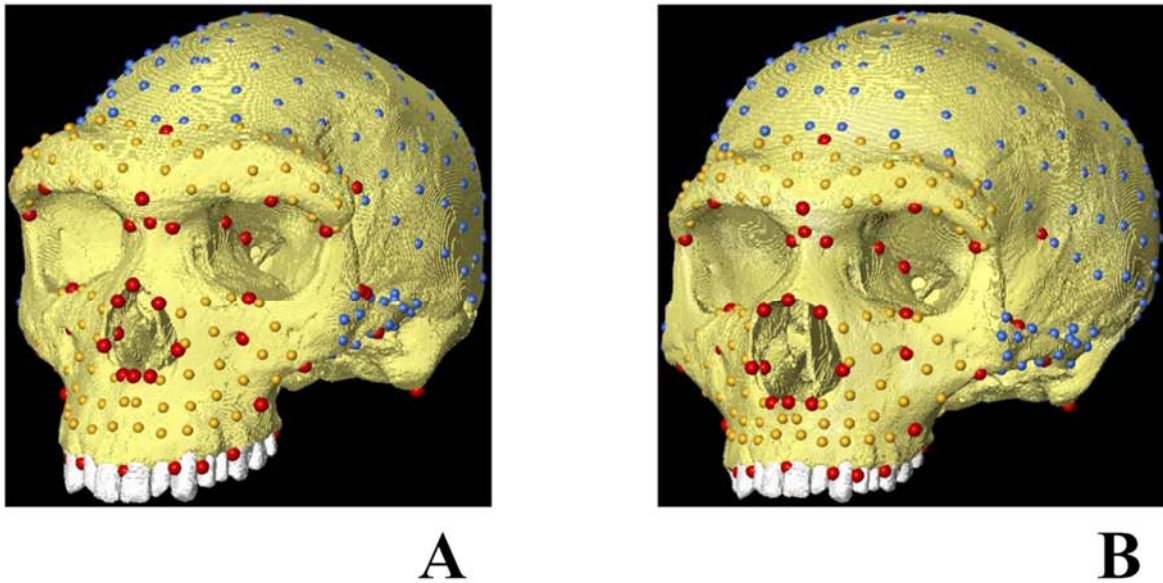
862

863 Figure 1: Cranium of Kabwe 1 (A) before and (B) after reconstruction.

864

865

866



867

868 Figure 2: A reconstructed Kabwe 1, *Homo heidelbergensis* cranium model (A) and a
869 hypothetical *Homo neanderthalensis* (B). The hypothetical Neanderthal was created via
870 surface warping model A into a mean Neanderthal landmark data set (B) using thin plate
871 splines based on classical and sliding semi-landmarks. Conventional landmarks (red spheres);
872 sliding semi-landmarks on the maxilla and brow-ridge (yellow spheres); sliding semi-
873 landmarks of the vault and zygoma (light blue spheres).

874

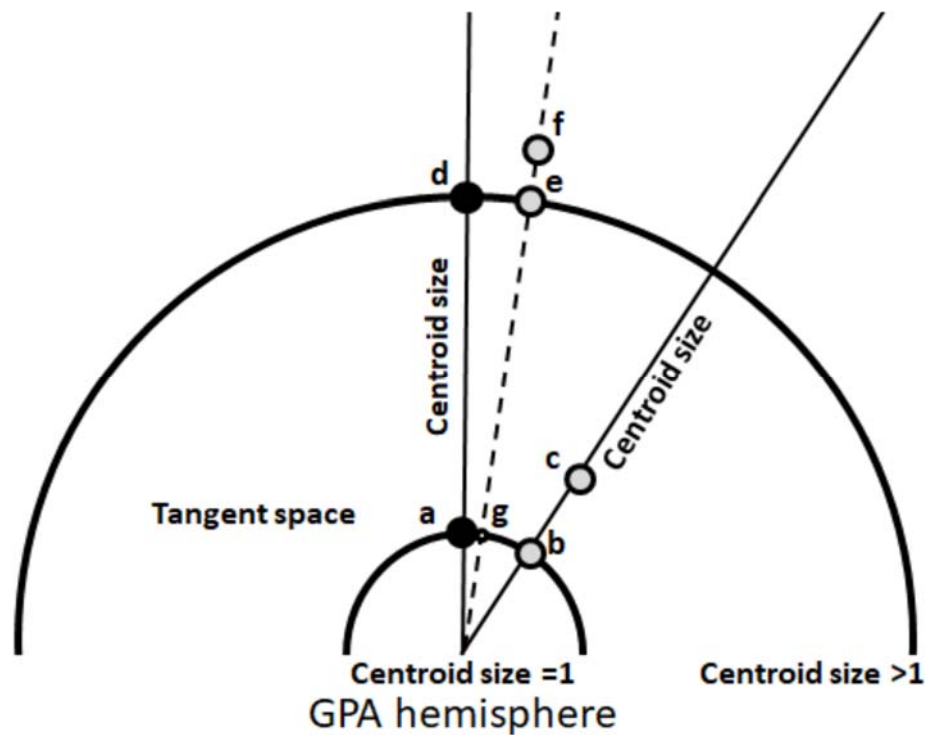


Figure 3: A schematic illustrating the hemisphere of GPA aligned coordinates (Slice 2001) for triangles, showing the tangent space, the vectors of centroid size, and the size and shape space resulting from rescaling of GPA registered coordinates to centroid size >1 . The black points, a and b, represent the same unloaded forms with different centroid sizes. The grey points c and f represent the loaded forms and the grey points b and e represent their projections onto the GPA hemispheres with centroid sizes $=1$ and >1 . G is the projection of f and e onto the GPA hemisphere with centroid size $=1$. See text for explanation.

900

901

902 Figure 4: PCA of large scale deformations of a sensitivity study assessing the impact of
903 simplifications of material properties in a modern human cranium. Model 1 is not visible
904 because it is in the same location in the plot as model 2. Deformations are magnified by a
905 factor of 500 to facilitate visualisation.

906

907